UNIVERSITY OF CALIFORNIA SAN DIEGO

Multiple Methods to Crystallize Quasi-2D Perovskites on Glass Substrate

A Thesis submitted in partial satisfaction of the requirements
for the degree Master of Science

in

Materials Science and Engineering

by

Zijing Wu

Committee in charge:

Professor Sheng Xu, Chair
Professor Renkun Chen
Professor Javier Garay

2023

The Thesis of Zijing Wu is approved, and it is acceptable in quality and form for publication on microfilm and electronically.

University of California San Diego

2023

TABLE OF CONTENTS

THESIS APPROVAL PAGE iii
TABLE OF CONTENTS iv
LIST OF FIGURES v
LIST OF TABLES vi
ACKNOWLEDGEMENTS vii
ABSTRACT OF THE THESIS iii
CHAPTER 1. Introduction 1
CHAPTER 2. Comparison of Surface Microstructure 5
CHAPTER 3. Comparison of Phase Distribution 10
CHAPTER 4. Comparison of Optoelectronic Properties 13
CHAPTER 5. Conclusion and Outlook 18
CHAPTER 6. Method 20
APPENDIX 23
REFERENCES 25

LIST OF FIGURES

Figure 2.1: The Scanning Electron Microscope (SEM) diagrams of different perovskite thin films based on DDM through (a) Origin, Additive-treatment: (b) Crown and (c) PEO, Antisolvent-treatment: (d) CB, (e) Tol and (f) EA and Hot-casting: (g) 80°C, (h) 100°C and (i) 120°C. The scale bar was 1μm. 8

Figure 2.2: The Scanning Electron Microscope (SEM) diagrams of different perovskite thin films based on RM through (a) Origin, Additive-treatment: (b) Crown and (c) PEO, Antisolvent-treatment: (d) CB, (e) Tol and (f) EA and Hot-casting: (g) 80°C, (h) 100°C and (i) 120°C. The scale bar was 1μm. 9

Figure 3.1: The X-ray Diffraction (XRD) patterns of different perovskite thin films based on DDM through (a) Additive-treatment and Origin, (b) Antisolvent-treatment and (c) Hot-casting. 12

Figure 3.2: The X-ray Diffraction (XRD) patterns of different perovskite thin films based on RM through (a) Additive-treatment and Origin, (b) Antisolvent-treatment and (c) Hot-casting. 12

Figure 4.1: The Photoluminescence (PL) spectra of perovskite thin films based on DDM with (a) Additive-treatment and Origin, (b) Antisolvent-treatment, (c) Hot-casting and (d) DDM Summary. 16

Figure 4.2: The Photoluminescence (PL) spectra of perovskite thin films based on RM with (a) Additive-treatment and Origin, (b) Antisolvent-treatment, (c) Hot-casting and (d) RM Summary. 17

LIST OF TABLES

Table 4.1 The Summary of PL spectra of perovskite thin films based on DDM. 16

Table 4.2: The Summary of PL spectra of perovskite thin films based on RM. 17

ACKNOWLEDGEMENTS

I would like to acknowledge Prof. Sheng Xu from Nanoengineering department in University of California, San Diego for providing all theoretical and technical support during these two years, helping me to grow up very fast. Also, as the chair of my committee, his valuable advice for my thesis helps me a lot.

I would also like to acknowledge Chengchangfeng Lu and Ruotao Wang for guiding all the experimental procedures and details to optimize the results. They inspired me a lot and gave me so many useful suggestions. Without them, I cannot finish my project and I cannot even find my present job.

ABSTRACT OF THE THESIS

Multiple Methods to Crystallize Quasi-2D Perovskites on Glass Substrate

by

Zijing Wu

Master of Science in Materials Science and Engineering

University of California San Diego, 2023

Professor Sheng Xu, Chair

As an innovative optoelectronic material, quasi-two-dimensional (quasi-2D) perovskite has attracted huge interests due to its high stability, easily tunable bandgap and high radiative recombination efficiency, making it a perfect candidate of solar cells, LEDs and other photovoltaic devices. Although basic information exists, this material lacks a systematic and comprehensive study. Current knowledge appears fragmented, making it essential to combine insights from various sources to develop a more thorough understanding of the subject. To gain deep understanding and precise control on the crystallization of quasi-2D perovskite, we successfully engineered quasi-2D perovskite thin films on glass substrate, employing two distinct methodologies: the Direct Dissolving Method (DDM) and Redissolving Method (RM). Moreover,

some of the sophisticated treatments were exerted on each method to enhance and optimize the film quality. We found that RM could possess a remarkable capability to synthesize thin films exhibiting reduced defects and superior phase purity with much lower crystallization rate when no extra treatments were applied. Concurrently, these advanced treatments were found to significantly enhance the film quality in various aspects, including surface microstructure, phase distribution, and optoelectronic properties, thereby contributing to an overall improvement of the films' quality and efficacy.

CHAPTER 1. Introduction

Since first being discovered in 1830s by Prof Gustavus, the perovskites with the structure of ABX_3 (X can be oxygen or halides) have gained strong interest for their low-cost processing with direct bandgap property. [1, 2]Among which, metal halide perovskites (MHPs), like 3D organic $CH_3NH_3PbBr_3$, $CH_3NH_3PbI_3$, or inorganic $CsPbBr_3$, [3]show their advantages of tunable bandgap, easy fabrication and defect tolerance. [4, 5]In such situation, they are exceptional candidates that can be applied in optoelectronic devices, like LEDs, lasers, and photovoltaics. [6-9]

Despite of these strengths, the traditional 3D MHPs (ABX_3) still have some limitations. The relatively long carrier diffusion length and small binding energy give rise to irradiative recombinations, which restricts their applications in light-emitting devices. [5, 10] Meanwhile, their tolerance to various environments, such as those with high moisture or temperature, is so poor that their use in industry is still negligible compared with more widely used silicon-based devices. [11, 12] To solve such problems, a series of spacers were introduced to create quasi-2D perovskites with the form like $A'_2A_{n-1}B_nX_{3n+1}$ in most of the cases, where A' generally is an organic amine cation, while A, B and X are monovalent cation (MA^+, FA^+ or Cs^+), divalent metal cation (Pb^{2+} or Sn^{2+}) and halide anion, respectively. [5, 11, 13, 14] This particular arrangement is recognized as the Ruddlesden–Popper (RP) crystal phase. With the interference of spacers, A sites are partially occupied through Van der Waal's interaction,[15] perovskite slabs [BX_6] are separated and multi-quantum-well (MQW) structures are formed. [16] Such structures, utilizing the quantum confinement effect and dielectric confinement effect, can not only improve the stability under wet or hot environments, [17] but also enhance exciton binding energy. [18, 19] Another remarkable strength of quasi-2D perovskites is that tuning their bandgap can be easily

realized. Changing the quantity of layers of perovskite slabs (n number) can help to modify the bandgap due to the quantum confinement effect. This situation allows for the adjustment of Photoluminescence (PL) and Electroluminescence (EL) wavelength ranging from the violet (400nm) to the near-infrared (780nm) regions by modifying the composition and ratio of precursors.[20-23] As a result, several groups utilize quasi-2D perovskites to fabricate high-efficiency optoelectronic devices. For instance, Zema et al. [24] combined quasi-2D perovskite $PEA_2PbBr_4(CsPbBr_3)_4$ with a typical additive ETPTA. As a result, the external quantum efficiency (EQE) of the fabricated perovskite LED (PeLED) could be over 22%. Zhe et al. [25] adopted dual-additive method, utilizing 18-crown-6 (Crown) with poly(ethylene glycol) methyl ether acrylate (MPEG-MAA), and the resulting LED achieved EQE over 28%. Ming et al. [26] mixed FA^+ with MA^+ in quasi-2D perovskites and the power conversion efficiency (PCE) of the resulting solar cell could be over 20%.

Even though some time has passed since quasi-2D perovskites was first synthesized, the processing technique is still restricted. The most common method is directly dissolving precursors in organic solution following stoichiometric ratio. However, the formation energy between quasi-2D perovskites having different n number is so limited that crystallized film tends to contain a variety of n-value phases even when they adhere to one specific stoichiometric ratio. [11, 23, 27] A energy-funneling process is formed in this case: the injected carriers will flow from larger bandgap (small-n) to smaller bandgap (large-n) phase, where they had recombinations. This process can increase photoluminescence quantum yield (PLQY), [28] but also leads to several drawbacks: This tendency restricts the energy of generated photons and the emission region, notably in deep-blue to violet range. Moreover, too many carriers gathering at large-n region can give rise to Auger recombination, which affect radiative recombination efficiency. [29] Numerous

treatments have been proposed during crystallization to enhance the purity and morphology of the film, such as adding antisolvent [30] and hot casting [29] , but the results have not been sufficiently compelling. Recently, a fascinating approach to hinder problems above was discovered, which was known as “Redissolving Method” (RM) [31] : Redissolve the grown single-crystalline quasi-2D perovskite in organic solution and then crystallize on substrates. Due to crystal growth process, the defects of perovskites are negligible even though the purity of precursors is limited. In comparison to the conventional “Direct Dissolving Method” (DDM), high purity and crystallinity, carefully managed crystal orientation, and desirable phase distribution are thus obtained. [32] Except for these two methods, several treatments are also applied in combination to further promote the film quality, like adding antisolvent or additive, or preheating the substrate and solution before crystallization. [30, 33, 34]

Herein, we utilized $PEA_2Cs_2Pb_3Br_{10}$ (n=3) as quasi-2D perovskites. As a typical spacer with a Benzene, PEA contains a strong degree of unsaturation due to its large π bond with high chemical activity and electron delocalization. [15] In order to distinguish these two main methods: DDM and RM, and improve the resulting film quality, we employed four common treatments for each method: Origin (pristine sample), Additive-treatment (18-Crown-6 (Crown) and Polyethylene oxide (PEO)), Antisolvent-treatment (Chlorobenzene (CB), Toluene (Tol) and Ethyl Acetate (EA)) and Hot-casting (80°C, 100°C and 120°C). After crystallizing on glass substrates, several characterizations have been used to analyze their optoelectronic and structural properties and surface morphologies based on both methods, like Scanning Electron Microscope (SEM), X-ray Diffraction (XRD) and Photoluminescence (PL) spectra. We have revealed that utilizing the innovative RM, it’s possible to synthesize the remarkably pristine thin films characterized by significantly restricted defects and high phase purity, while maintaining a much lower

crystallization rate. Employing three alternative treatments, we observed a discernible enhancement in the film quality, manifesting in diverse aspects such as improved surface microstructure, more uniform phase distribution, and superior optoelectronic properties.

CHAPTER 2. Comparison of Surface Microstructure

DDM was utilized to synthesize quasi-2D perovskite thin films through four treatments mentioned above. The perovskite solution was made by totally dissolving precursors in dimethyl sulfoxide (DMSO) following stoichiometric ratio (see **Method**). Moreover, these four treatments were also exerted on quasi-2D perovskite films based on RM, and these films were tested in similar ways. The single quasi-2D perovskites were synthesized by acid precipitation method [35] (see **Method**): PEABr, $PbBr_2$ and PbO were totally dissolved in preheated HBr in stoichiometric ratio, then slowly brought the solution down to room temperature. During this process, the bright yellow flakes were gradually precipitated, which were the single crystals needed (Fig. A1). After cleaning, the flakes were redissolved in organic solution for further use. Before exploring the characterization results, a key difference between DDM and RM was that RM showed a relatively lower crystallization rate according to spin-coating process. Additionally, such phenomenon helped these treatments to demonstrate their influence more fully on quasi-2D perovskites and further improved the thin film quality.

Firstly, an in-depth analysis of the morphology of each thin film was conducted. Figure 2.1 and Figure 2.2 showed the images of Scanning Electron Microscopy (SEM) of samples subjected to various treatments based on different methods. Due to relatively slower crystallization rate during spin-coating, RM tended to form thin films with higher quality with sufficient time. To elaborate further, without any treatments, the surface microstructure defects of the pristine films based on RM were considerably restricted when compared to those synthesized via DDM, revealing a more uniform grain size and more regular grain shape according to SEM (Fig. 2.1a and Fig. 2.2a).

Then, two distinct additives were introduced as a treatment to improve the film quality. Additives are typically large or small organics with sufficient oxygen atoms. These atoms can form hydrogen bond with amino-group in some spacers, like Phenethylamine (PEA), to suppress the gathering of PEABr and get the desired fixed n-phase perovskites. [33] Moreover, additives can temporarily combine with [$PbBr_6$] perovskite slabs to restrict dangling bond, effectively passivating the defects and making the crystallization and size distribution more controllable. Obviously, both methods utilizing Additive-treatment could generate thin films with more uniform grain size around 200-300nm, as illustrated in Figure 2.1b, c and Figure 2.2b, c, while the grain size of pristine samples ranged from tens to hundreds of nanometers. Xiang et al. [36] linked grain size from SEM to n number phases. They believed that the existence of larger n phases could account for the observed larger grain sizes. According to their research, herein pristine samples showed the existence of different n phases. Furthermore, the defects could also be limited with the help of these additives. Nevertheless, the dissimilarities also existed between these two methods despite employing the same additives. As a characteristic short chain additive, Crown could evidently help to regulate the film morphology and suppress pinholes and defects in both methods (Fig. 2.1b and Fig. 2.2b). However, the enhancement of the film quality utilizing PEO was not as clear as that taking use of Crown when employing DDM, with even more pinholes than the pristine sample had (Fig. 2.1c). Such limitation could be attributed to insufficient reaction between this long chain additive and perovskites during spin-coating due to the rapid crystallization process, which potentially hindered the desired interaction and incorporation of the additive. On the contrary, the thin films based on RM presented a minor difference when treated by these two additives. Moreover, because of sufficient crystallization time, grains began to accumulate and formed larger grains with size up to several micrometers (Fig. 2.2 b, c).

In the case of Antisolvent-treatment, a shared characteristic observed for both methods were that the grain size of films was the smallest with excellent coverage and flatness (Fig. 2.1 d-f and Fig. 2.2 d-f), which could be ascribed to the enhanced presence of low-n phases. [36] With the help of antisolvent, the host solvent can be removed in a short time and crystallization process can be accelerated to restrict defects and form high quality films. [30] Meanwhile, the rapid decrease of solubility helped more spacers to precipitate, which subsequently combined with perovskites. Furthermore, RM could generate thin films with smoother surface and larger grain size, as illustrated in Figure 2.2d-f. According to the XRD patterns analyzed later (Fig. 3.2b), these larger grains belonged to quasi-2D perovskites with n=1 phases, and the existence of these phases could remarkably raise the bandgap due to quantum confinement effect. Nevertheless, much faster crystallization rate DDM caused could make more precursors crystallize before contacting with antisolvents so that their role was limited, causing much fewer spacers being isolated from solution and combining with [$PbBr_6$] slabs. Furthermore, their grains were too small to recognize.

When we investigated Hot-casting, the situation was totally different. According to the literature, hot casting can also accelerate the crystallization process with adequate thermal energy and get rid of the influence of intermediate phase. [34] In our experiment, we noticed that when casting temperature was relatively low (Fig. 2.1g and Fig. 2.2g), the surface was still continuous even though the flatness was not so good, with undulating surface looking like a mountain. This phenomenon had the potential to restrict the quality of perovskite films. When the casting temperature was raised up, the surface of the film became less successive, regular microcrystals with square shape appeared and they looked like the initial process of single-crystalline formation, [37] but the size of each microcrystal was limited, as illustrated in Figure 2.1h and Figure 2.2h. Both the film discontinuousness and crystal size were increased when further improved casting

temperature (Fig. 2.1i and Fig. 2.2i) due to enough thermal energy for formation. Such phenomenon would appear more obviously when we continued to increase the casting temperature to 140°C (Fig. A2), most of the crystals became isolation with their size up to several hundred nanometers when utilizing both methods. To sum up, for Hot-casting treatment, higher casting temperature could lead to larger crystal size with more separated surface microstructure. Despite these similarities, discernible differences persisted. The crystallization process associated with RM exhibited a much slower progression, attributable to a significantly reduced crystallization rate. To be more specific, most of the grains didn't begin to separate until the casting temperature reached 120°C when utilizing RM. In contrast, DDM facilitated the isolation of most grains at a lower temperature of 100°C.

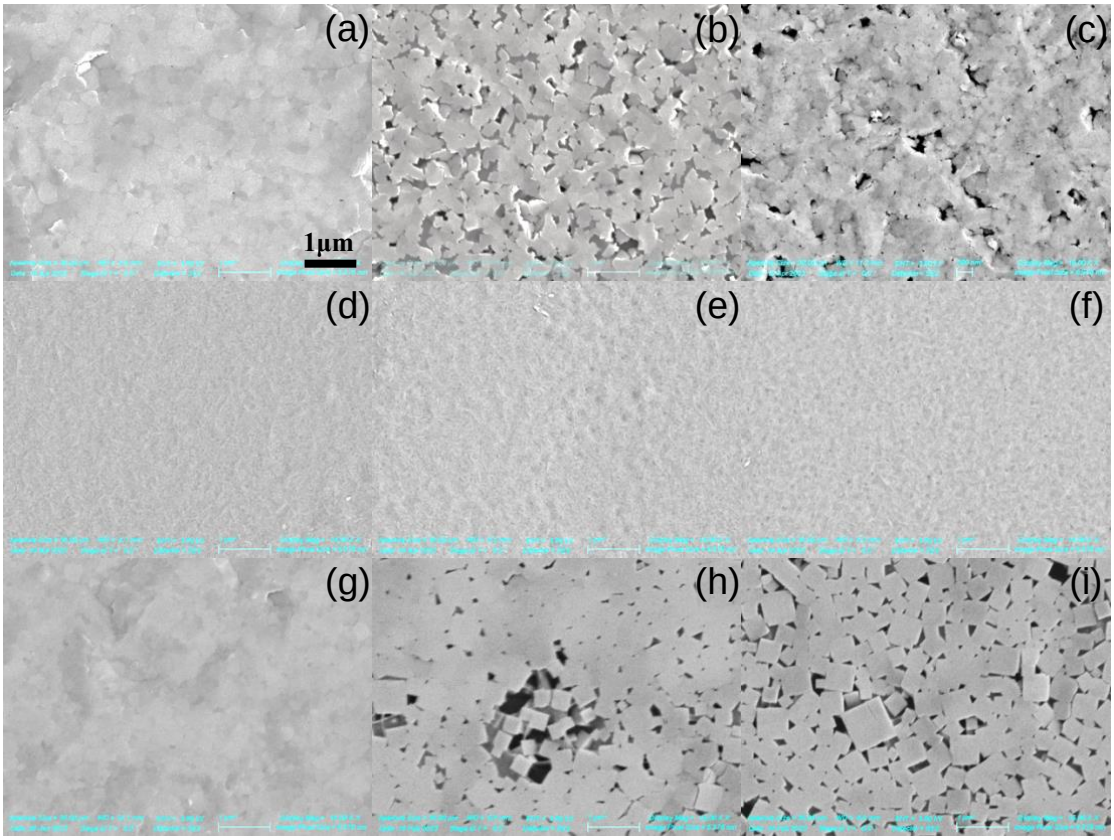

Figure 2.1: The Scanning Electron Microscope (SEM) diagrams of different perovskite thin films based on DDM through (a) Origin, Additive-treatment: (b) Crown and (c) PEO, Antisolvent-treatment: (d) CB, (e) Tol and (f) EA and Hot-casting: (g) 80°C, (h) 100°C and (i) 120°C. The scale bar was 1μm.

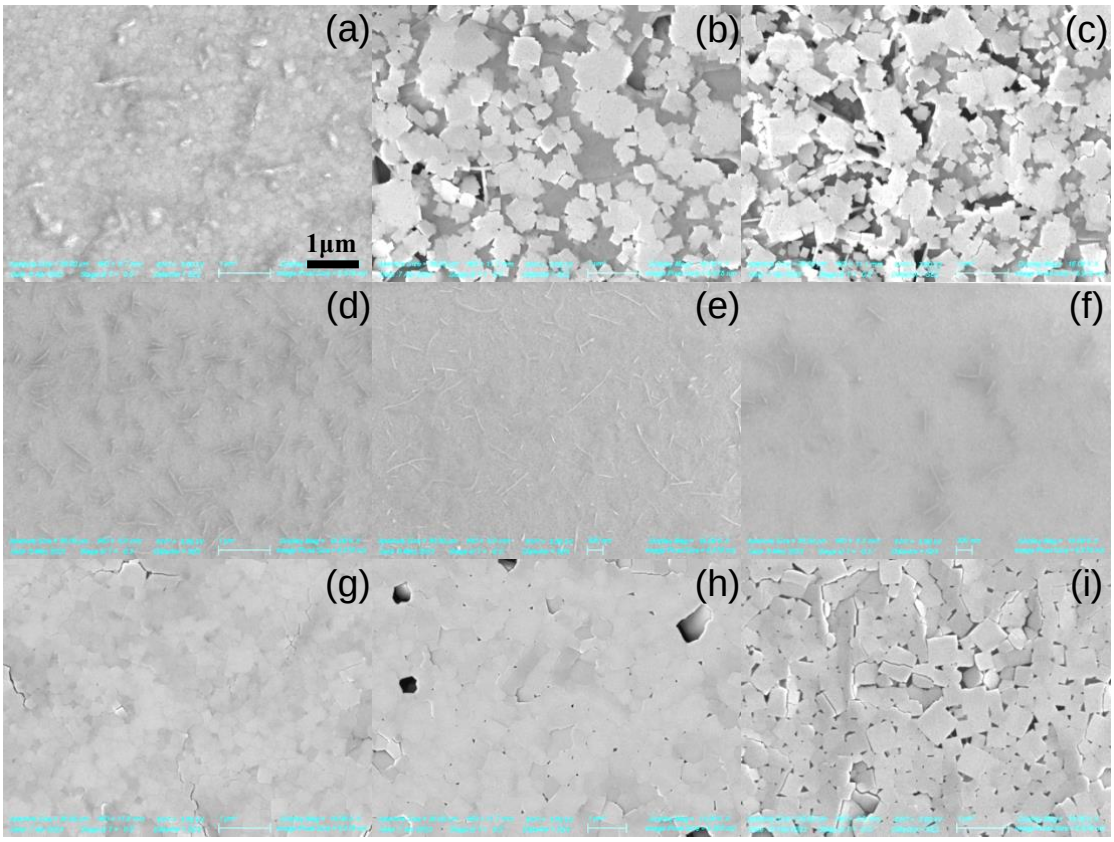

Figure 2.2: The Scanning Electron Microscope (SEM) diagrams of different perovskite thin films based on RM through (a) Origin, Additive-treatment: (b) Crown and (c) PEO, Antisolvent-treatment: (d) CB, (e) Tol and (f) EA and Hot-casting: (g) 80°C, (h) 100°C and (i) 120°C. The scale bar was 1μm.

CHAPTER 3. Comparison of Phase Distribution

Except for the morphology, another crucial factor to consider is the crystallinity. Quasi-2D perovskites have a propensity that can produce phases with varying n-values, even following the stoichiometric ratio. As a result, developing strategies to enhance the phase purity is a critical challenge to be solved. Herein, the X-ray diffraction (XRD) measurements were applied to characterize the phase distribution of each thin film.

Firstly, several similarities were identified in the XRD patterns. The main peaks below 10° proved the existence of quasi-2D perovskites and these peaks corresponded to (002) planes. [38] We could tell that there were two set of peaks. Firstly, a set of peaks with the equal space (at ~5.3°, 10.6°, 15.9°, 21.3°, 26.7° and 32.2°) represented the parallel planes of (00x), where x was even. These planes were spaced by spacers with the tendency of out-of-plane orientation and confirmed the presence of PEA_2PbBr_4 (n=1). The interplanar distance between the (00x) planes could be calculated as ~1.67nm from Bragg's equation. Then, some of the patterns had the peaks at ~15.2° and 30.6°. This set of peaks correlated with (100) and (200) planes generated by $CsPbBr_3$. [38]

The pristine samples synthesized via these two methods were then analyzed to show the possible difference in crystal structure. The XRD patterns revealed that even though both methods could lead to peaks at the same positions, their relative intensity varied. Apparently, the peaks representing (100) and (200) planes were greatly enhanced when RM was exerted, as shown in Figure 3.1a and Figure 3.2a. The enhancement implied the increased amount of Cs^+ in quasi-2D perovskites. Therefore, phases was further regulated with more large n number phases being yielded.

Moreover, the phase distribution of the thin films adding additives were meticulously investigated through XRD. Obviously, the incorporation of both additives led to a more significant enhancement of the peaks at approximately 15.2° and 30.6° in comparison to the pristine samples (Fig. 3.1a and Fig. 3.2a), suggesting that an increased concentration of Cs^+ contacted and reacted with quasi-2D perovskites as well and generated a greater number of n>1 phases. The addition of these additives facilitated a more controlled phase distribution. Both Crown and PEO could cause the analogous results with minor difference.

Three antisolvents were introduced as well to investigate their influence on crystallinity, and a very sharp change occurred. When utilizing DDM, the peaks were distributed randomly and only parts of the equidistant peaks appeared, as shown in Figure 3.1b. Also, the intensity of peaks was so weak with relatively broad FWHM. These all implied a poor crystallinity. According to the SEM images mentioned above (Fig. 2.1 d, e, f), the grains were hard to recognize owing to their small size. This observation correlated with the weak XRD peaks. RM could generate quasi-2D perovskites with more regular phases. With the help of antisolvent, the characteristic peaks corresponding to $CsPbBr_3$ (at ~15.2° and 30.6°) were eliminated, resulting in the presence of uniformly spaced peaks from PEA_2PbBr_4 (Fig. 3.2b). This meant that the n>1 phases were intensely restricted and the dominant perovskites were PEA_2PbBr_4, equivalent to what SEM presented. Nevertheless, those equidistant peaks correlating with PEA_2PbBr_4 illustrated very low intensity and broad peak width as well, showing relatively poor crystallinity.

We also employed Hot-casting to study its effect. Evidently, the resulting XRD patterns were similar with what Additive-treatment could cause: The relative enhancement of peaks at approximately 15.2° and 30.6° suggested an increased prominence of phases with higher n-values. Moreover, RM made quasi-2D perovskites exhibit a unique temperature-dependent trend.

Compared with quasi-2D perovskites based on DDM (Fig. 3.1c), those peaks generated by $CsPbBr_3$ were enhanced more powerfully of those synthesized via RM when increasing casting temperature (Fig. 3.2c).

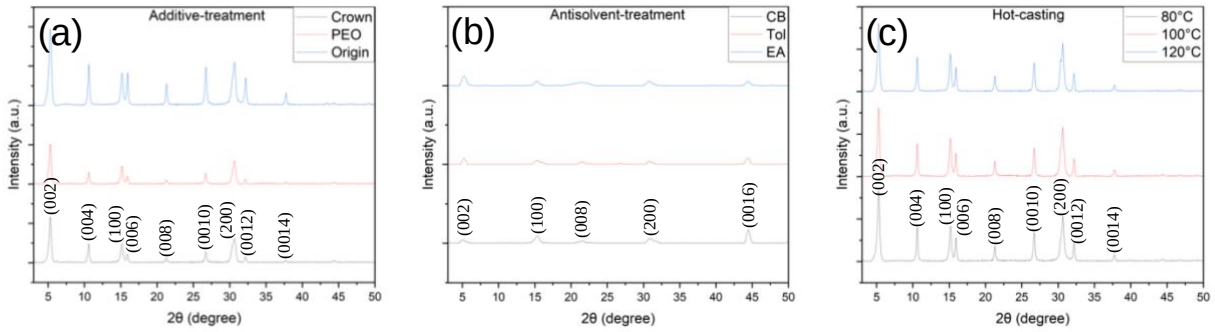

Figure 3.1: The X-ray Diffraction (XRD) patterns of different perovskite thin films based on DDM through (a) Additive-treatment and Origin, (b) Antisolvent-treatment and (c) Hot-casting.

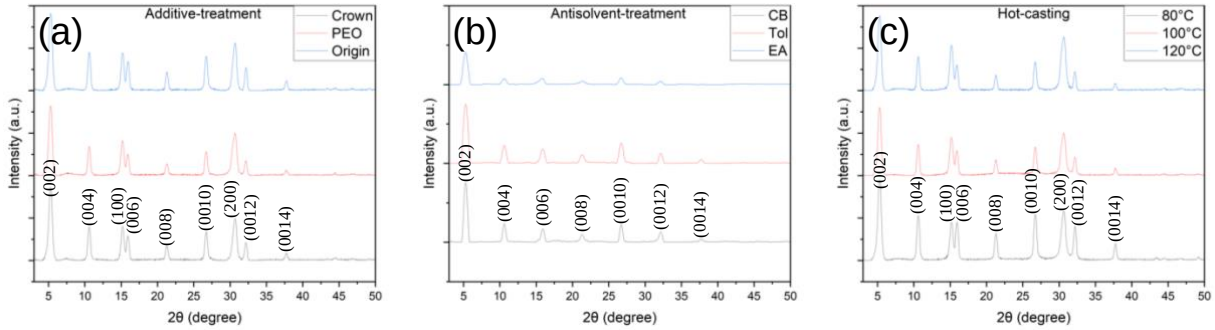

Figure 3.2: The X-ray Diffraction (XRD) patterns of different perovskite thin films based on RM through (a) Additive-treatment and Origin, (b) Antisolvent-treatment and (c) Hot-casting.

CHAPTER 4. Comparison of Optoelectronic Properties

As a competitive material for optoelectronic devices, like LEDs, lasers and photodetectors, the optoelectronic properties of the quasi-2D perovskite are also essential to investigate. Therefore, the Photoluminescence (PL) spectra of the quasi-2D perovskite thin films based on two methods were meticulously assessed and analyzed to assess the effects of the various treatments on their optoelectronic properties. Furthermore, the peak position and Full Width at Half Maximum (FWHM) of PL were summarized in Table 4.1 and Table 4.2. According to our summary, the blueshift of the PL peak in pristine samples demonstrated the reduction of defects in the thin films fabricated using the Redissolving Method (RM), indicating an improvement in film quality and characteristics. (Table 4.1 and 4.2).

For Additive-treatment, the PL intensity was strongly enhanced compared with pristine samples when exerting both methods, which was constant with more uniform grain size and fewer pinholes and defects as SEM images revealed (Fig. 4.1a and Fig. 4.2a), apparently reforming the purity and quality of perovskite thin film. Moreover, all peaks treated by additives had a blueshift due to the restriction of defects (Table 4.1 and 4.2), and the narrow FWHM observed in this case signified the high purity of the thin films obtained. To analyze separately, however, PEO had much less contribution on optical properties than Crown did for the thin films synthesized via DDM, as illustrated in Figure 4.1a. This observation was correlated with the limitations in the film quality. The situation was varied for the samples generated by RM. Due to the formation of intermediate phase between oxygen atoms in additives and spacers in perovskites, it took more time for the samples treated by additives to crystallize compared with pristine samples. Furthermore, samples based on RM exhibited a significantly slower crystallization rate compared to those synthesized

by DDM even when utilizing the same additive. For PL diagram of pristine sample, the small peak at 425nm represented the existence of n = 2 phase, and both additives clearly decreased this peak, while Crown had a more efficient influence (Fig. 4.2a). Nevertheless, unlike the effect of DDM, both Crown and PEO could lead to PL peaks with almost the same peak intensity when employing RM. As mentioned before, as a typical long chain additive, PEO required more time to react with perovskites and form intermediate phases compared with short chain Crown, so that longer crystallization time could let PEO sufficiently affect the thin films and get better quality.

Then, the effects of the antisolvents were investigated as well. Like Additive-treatment, antisolvent could significantly increase the PL intensity, as shown in Figure 4.1b and Figure 4.2b. Moreover, the much greater blueshift with the help of Antisolvent-treatment was caused by the generation of a boost quantity of phases with small n-value, which intensely enhanced the bandgap of quasi-2D perovskite (Table 4.1 and 4.2). To elucidate, the introduction of antisolvent effectively promoted the precipitation of spacers so that more spacers were combined with $[PbX_6]$ slabs in a short time. The small FWHM here presented the high purity of thin films obtained. However, it's worth noting that the tool utilized for RM here was different from that for DDM upon adding antisolvents after spin-coating. Traditionally, pipette was the main tool used for this treatment. However, due to its unique structure, the solution was crushed onto the substrate other than dropped onto it during spin-coating. As a result, there was a possibility that part of the uncrystallized solution would be flushed away and causing nonuniform crystallization, especially with a relatively low crystallization rate. According to images of synthesized films using pipette (Fig. A3a), the color of the center part was lighter than other part around the center, which proved the hypothesis. To handle this problem, we took advantage of syringe other than pipette as the tool so that the antisolvent could be added more gently and got a film with high quality (Fig. A3b). The

insert SEM images indicated morphologies from different tools, where the syringe achieving better flatness and coverage likewise. What's more, the PL spectra of the films fabricated through these two tools were also distinct. (Fig. A4a, b, c) As may be appreciated, the spacers could be more fully retained through syringe and more low n phases could form, leading to a blueshift. Meanwhile, the raised intensity proved the enhancement of film quality. However, the difference of the thin films treated by these two tools was negligible based on DDM (Fig. A4d), since higher crystallization rate could significantly limit this phenomenon.

Samples treated by Hot-casting showed some unique phenomena in SEM images, and these were also presented in PL spectra. Unfortunately, the results based on Hot-casting were not so satisfied and deep mechanisms should be thoroughly figured out (Fig. 4.1c and Fig. 4.2c). According to the SEM diagrams mentioned before, either the much rougher film at relatively low temperature or the discontinuous film surface upon higher casting temperature could be detrimental to the optical properties, leading to poor PL intensity. Furthermore, the nonuniform crystal size gave rise to several isolated peaks when being activated during testing, reflecting the poor purity of perovskite film (from ~415nm to ~ 610nm). Then, the peak position here showed an opposite tendency: an obvious redshift was observed upon being heated up. The increase of casting temperature gave rise to both larger grain size and higher-n phases with sufficient formation energy, which led to the redshift. [39] In addition, it's noteworthy that there were two main peaks here, which represented two main different phases. Besides, with the increase of casting temperature, the peak at larger wavelength could be higher, which could as well prove the explanation above. The relatively larger FWHM also implied the poor purity and quality of the thin films utilizing Hot-casting.

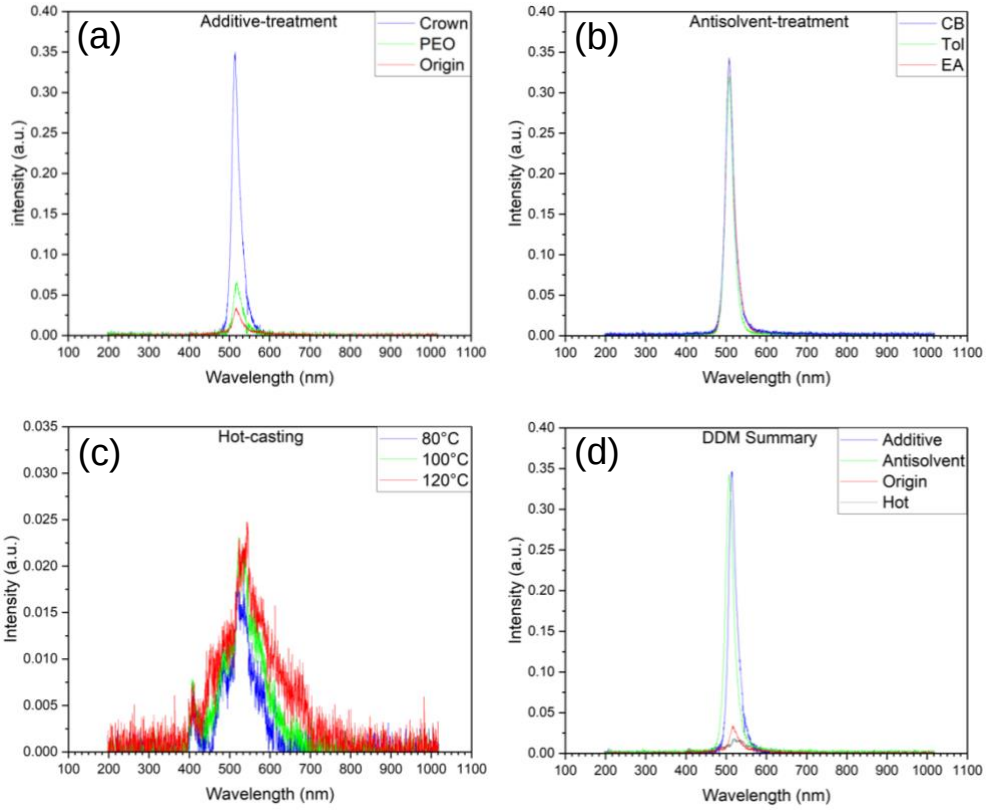

Figure 4.1: The Photoluminescence (PL) spectra of perovskite thin films based on DDM with (a) Additive-treatment and Origin, (b) Antisolvent-treatment, (c) Hot-casting and (d) DDM Summary.

Table 4.1 The Summary of PL spectra of perovskite thin films based on DDM.

	Peak position (nm)	FWHM (nm)
Additive-treatment	516	20
Antisolvent-treatment	507	22
Origin	518	21
Hot-casting	521/537	40

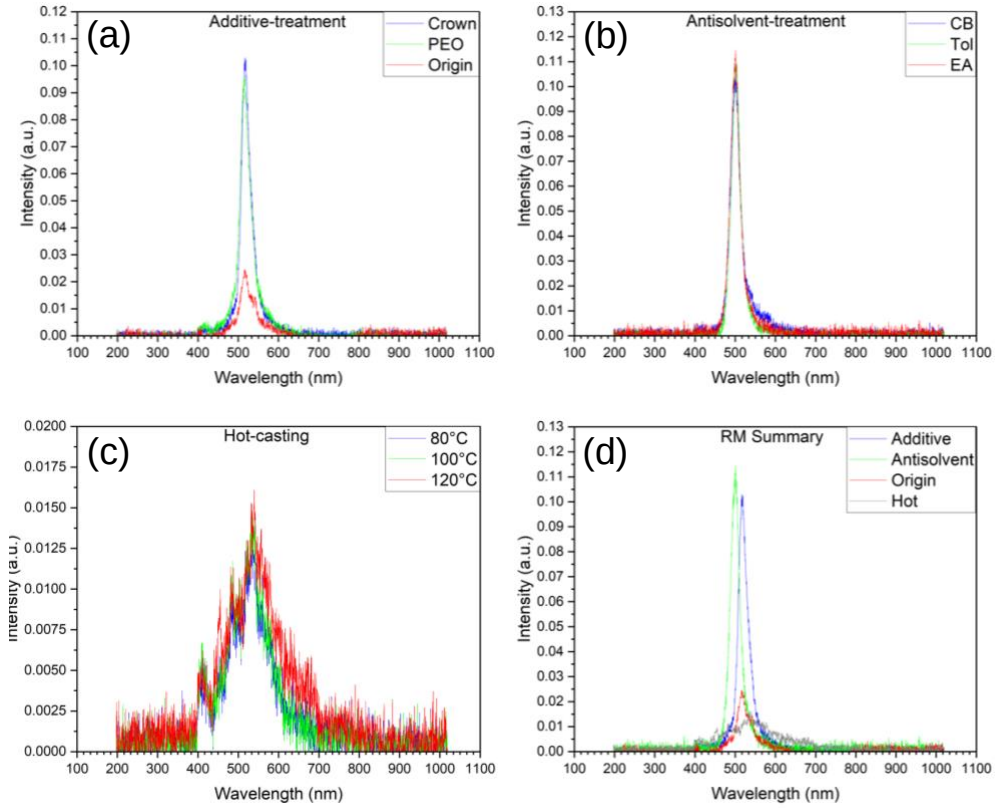

Figure 4.2: The Photoluminescence (PL) spectra of perovskite thin films based on RM with (a) Additive-treatment and Origin, (b) Antisolvent-treatment, (c) Hot-casting and (d) RM Summary.

Table 4.2: The Summary of PL spectra of perovskite thin films based on RM.

	Peak position (nm)	FWHM (nm)
Additive-treatment	514	26
Antisolvent-treatment	501	24
Origin	516	25
Hot-casting	521/540	42

CHAPTER 5. Conclusion and Outlook

To sum up, we showcased the quasi-2D perovskite thin films based on two different methods, DDM and RM, through different treatments, and analyzed and compared the influence of each treatment on these two methods. The morphology, phase distribution and optoelectronic properties were thoroughly studied through SEM, XRD and PL measurements. We figured it out that thin films synthesized via RM had much slower crystallization process compared with those based on DDM. As a result, this facilitated the treatments to present their impact more effectively on quasi-2D perovskites, leading to a further enhancement of the thin film quality. Such phenomenon gave rise to grains with larger size when thin films were treated by additives utilizing RM. Moreover, due to sufficient reaction time, RM could make PEO synthesize samples with comparable quality to those obtained by Crown, which was on both surface microstructure and optoelectronic properties. Then, to preserve the maximum amount of precursor solution, it's necessary to employ a distinct tool for the introduction of antisolvent to thin films synthesized via RM to optimize film quality. As a result, quasi-2D perovskites with smoother surface, larger grain size and more regular phase distribution were obtained. Furthermore, during the hot casting process, the morphology of thin films produced by RM exhibited a more delayed response to the casting temperature in comparison to those obtained using DDM. Moreover, thin films based on RM presented a unique temperature-dependent trend in phase distribution. Apparently, the great restriction of pinholes and defects and relatively pure phase distribution made RM a promising method to synthesize perovskite thin films with high quality and with multiple compositions to fabricate photovoltaic devices with high efficiency.

Undoubtedly, the study on quasi-2D perovskite thin film is far from enough. Many of the research didn't clearly distinguish RM and DDM during crystallization and their differences were rarely mentioned. Even though several treatments have been studied with different parameters, more factors can be changed for further study. For example, more types of antisolvents or additives, different concentration of additives or more different casting temperature can give rise to different film qualities. Also, some fixed parameters in our experiment during spin-coating and annealing can also be adjusted to optimize the film quality, including the concentration of quasi-2D perovskite solution. There is no doubt that different treatments require different film thickness or crystallization temperature to maximize their effects. What's more, more characterizations are needed to dig deep into the intrinsic properties of these quasi-2D perovskite thin films, like crystal orientation, phase stability and structural arrangement. This promising material deserves more interests and attention.

CHAPTER 6. Method

Materials. All the materials were directly utilized without further treatment and stored in a N_2-filled glove box. CsBr (99%) and PbO (99.9%) were obtained from Alfa Aesar, and $PbBr_2$ (98+%) was purchased from Thermos Scientific. PEABr was obtained from GreatCell Solar, while the rest of chemicals were all purchased from Sigma-Aldrich, including DMSO and all the additives and antisolvents.

Quasi-2D perovskite single crystal growth. Here, $PEA_2Cs_2Pb_3Br_{10}$ (n=3) single crystalline perovskites were synthesized by acid precipitation method [39]: For precursors, PEABr (0.808g) and CsBr (0.852g) were dissolved together in preheated 5ml HBr, while PbO was dissolved in another 10ml HBr, and the dissolving temperature was 170°C. Both solutions became pale orange after totally dissolving the precursors. Then these two solutions were quickly mixed at the same reaction temperature, and little light-yellow flakes were generated right after combination. When slowly decreased the solution temperature, both the size and amounts of flakes increased. Two hours later, after reaching room temperature, supernatant was removed and leaving precipitation, which were the desired single crystals. To clean up, the remaining flakes were rinsed by Isopropyl Alcohol (IPA) by suction filtration for three to four times and were dry at 80°C afterwards to remove extra IPA. During this process, the color of these products became darker, turning into light orange. After cleaning, the needed quasi-2D perovskite single crystals were stored in a clean vial for later use.

Perovskite solution synthesis. The concentration of quasi-2D perovskite solution were fixed at 0.5M for both methods (In terms of C_{Pb}). For DDM, PEABr (67.03mg/ml), CsBr (70.94mg/ml) and $PbBr_2$ (183.5mg/ml) were dissolved in DMSO following the molar ratio of 2:2:3

in glove box, then sonicated for 15 minutes for complete dissolution. For RM, the pre-prepared quasi-2D single crystals were redissolved in DMSO with the concentration of 322mg/ml in glove box as well. The flakes could be easily dissolved in DMSO even without sonication or stirring.

Perovskite thin film synthesis on glass substrate. The glass (L×W×H was 15mm×20mm×1nm) substrates were sonicated in sequence of detergent powder, acetone, isopropyl alcohol and deionized water for 10 minutes each. After cleaning, the substrates were dried through gas flow and then treated by UV ozone for 15 minutes to activate surface free radicals and remove potential contamination. After that, the substrates were transformed into a nitrogen-filled glove box for further use. For Additive-treatment, Crown and PEO were added into DMSO in the concentration of 10mg/ml first. It's worth noting that, the melting point of Crown is too low that it's difficult to weigh this additive as a solid. To solve this, Crown can be preheated to melt and use pipette to add it into organic solution afterwards. PEO solution should be heated up to 50°C and be stirred overnight to get pure solution. After dissolving, the additive solution was mixed with perovskite solution in the ratio of 2:3 to get a perovskite solution with additive concentration of 4mg/ml. Then this solution was spin-coated on pre-treated glass substrate. After treatment, Crown could transfer the film color to green while PEO made the film look more blurred. For Antisolvent-treatment, one hundred microliters of each antisolvent were dropped onto the substrate 20s after spin-coating began continuously. Right after dropping, the film color immediately changed from yellow to bright green. Meanwhile, it's noteworthy that when treating RM, antisolvent should be added by syringe rather that pipette to retain perovskite solution and improve film quality. For Hot-casting, solution based on both methods was preheated at 80°C for 20 minutes before crystallizing. The substrates were also preheated at desired temperature (80°C, 100°C and 120°C) for 10 minutes before spin-coating. After heating up, the solution was directly

dropped onto hot substrate within 10s and the amount of solution should be large enough to cover the whole substrate so that the crystallization process could be more uniform. The color changed more quickly compared with the pristine sample during spin-coating, presenting the acceleration of crystallization. Also, the center part of the film was lighter in color than the surrounding parts after crystallization. It's worth noting that if the solution was preheated more than 30 minutes, the solution could become light brown and the resulting thin film tended to achieve a worse quality. All the spin-coating were at the speed of 4000rpm with 2000rpm acceleration, and RM required more time to crystallize than DDM. Right after spin-coating, the films were annealed at 80°C for 10 minutes to remove residue solution.

Characterization. The surface microstructure of quasi-2D perovskite thin films was collected by a Zeiss Sigma 500 scanning electron microscope with an acceleration voltage of 3kV and magnification of ×16k. The samples were attached to standard SEM base with conductive adhesive. XRD patterns were carried out by a Rigaku Smartlab X-ray diffraction using a $\theta/2\theta$ system with the scanning angle from 3° to 50° and using CuKα (λ = 1.542 Å) as X-ray source. Photoluminescence (PL) spectra were measured by M340F4 0.45 mW (Min) Fiber-Coupled LED from ThorLabs as excitation light source and CCS200 compact spectrometer from ThorLabs as detector. The wavelength of excitation light was 340nm.

APPENDIX

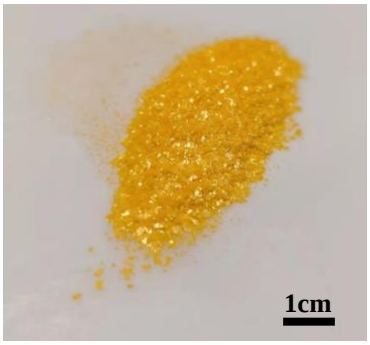

Figure A1. The $PEA_2Cs_2Pb_3Br_{10}$ (n = 3) quasi-2D perovskite single crystals synthesized by acid precipitation method. The scale bar was 1cm.

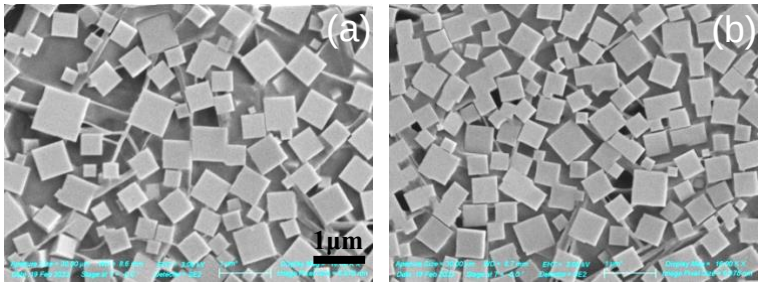

Figure A2. The scanning electron microscope (SEM) diagrams of quasi-2D perovskite thin film based on (a) DDM and (b) RM through Hot-casting with casting temperature at 140°C. The scale bar was 1μm.

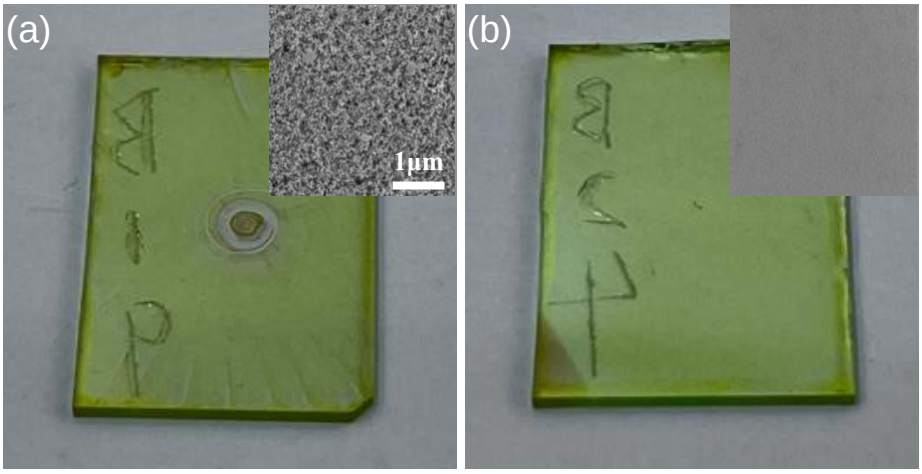

Figure A3. The pictures of thin films using (a) pipette and (b) syringe to add antisolvent during spin-coating based on RM. The insert diagrams are SEM of thin films using different tools based on RM. The scale bar was 1μm.

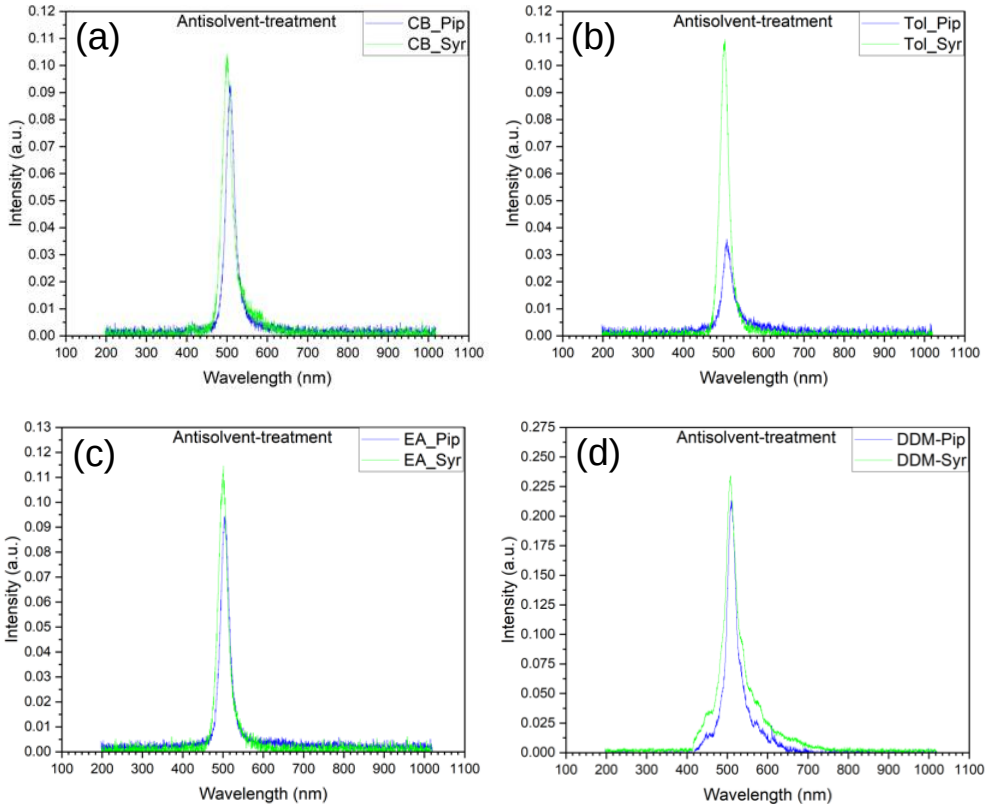

Figure A4. The PL spectra for the comparison of utilizing different tools when adding (a) CB, (b) Tol and (c) EA as antisolvent during spin-coating through RM, and adding antisolvent through (d) DM during spinning-coating.

REFERENCES

1. Ban, M., Zou, Y., Rivett, J. P. H., Yang, Y., Thomas, T. H., Tan, Y., Song, T., Gao, X., Credgington, D., Deschler, F., Sirringhaus, H., & Sun, B. (2018). Solution-processed perovskite light emitting diodes with efficiency exceeding 15% through additive-controlled nanostructure tailoring. Nature Communications, 9(1), 3892.

2. Bhalla, S., Melnekoff, D. T., Aleman, A., Leshchenko, V., Restrepo, P., Keats, J., Onel, K., Sawyer, J. R., Madduri, D., Richter, J., Richard, S., Chari, A., Cho, H. J., Dudley, J. T., Jagannath, S., Laganà, A., & Parekh, S. Patient similarity network of newly diagnosed multiple myeloma identifies patient subgroups with distinct genetic features and clinical implications. Science Advances, 7(47), eabg9551.

3. Blancon, J.-C., Even, J., Stoumpos, C. C., Kanatzidis, M. G., & Mohite, A. D. (2020). Semiconductor physics of organic–inorganic 2D halide perovskites. Nature Nanotechnology, 15(12), 969-985.

4. Chen, Y., Sun, Y., Peng, J., Tang, J., Zheng, K., & Liang, Z. (2018). 2D Ruddlesden–Popper Perovskites for Optoelectronics. Advanced Materials, 30(2), 1703487.

5. Chen, Y., Yu, S., Sun, Y., & Liang, Z. (2018). Phase Engineering in Quasi-2D Ruddlesden–Popper Perovskites. The Journal of Physical Chemistry Letters, 9(10), 2627-2631.

6. Chu, Z., Ye, Q., Zhao, Y., Ma, F., Yin, Z., Zhang, X., & You, J. (2021). Perovskite Light-Emitting Diodes with External Quantum Efficiency Exceeding 22% via Small-Molecule Passivation. Advanced Materials, 33(18), 2007169.

7. Chu, Z., Zhao, Y., Ma, F., Zhang, C.-X., Deng, H., Gao, F., Ye, Q., Meng, J., Yin, Z., Zhang, X., & You, J. (2020). Large cation ethylammonium incorporated perovskite for efficient and spectra stable blue light-emitting diodes. Nature Communications, 11(1), 4165.

8. Di, J., Chang, J., & Liu, S. (2020). Recent progress of two-dimensional lead halide perovskite single crystals: Crystal growth, physical properties, and device applications. EcoMat, 2(3), e12036.

9. Dong, W., Zhang, X., Yang, F., Zeng, Q., Yin, W., Zhang, W., Wang, H., Yang, X., Kershaw, S. V., Yang, B., Rogach, A. L., & Zheng, W. (2022). Amine-Terminated Carbon Dots Linking Hole Transport Layer and Vertically Oriented Quasi-2D Perovskites through Hydrogen Bonds Enable Efficient LEDs. ACS Nano, 16(6), 9679-9690.

10. Feng, W., Liao, J.-F., Chang, X., Zhong, J.-X., Yang, M., Tian, T., Tan, Y., Zhao, L., Zhang, C., Lei, B.-X., Wang, L., Huang, J., & Wu, W.-Q. (2021). Perovskite crystals redissolution strategy for affordable, reproducible, efficient and stable perovskite photovoltaics. Materials Today, 50, 199-223.

11. Green, M. A., Ho-Baillie, A., & Snaith, H. J. (2014). The emergence of perovskite solar cells. Nature Photonics, 8(7), 506-514.

12. He, Z., Liu, Y., Yang, Z., Li, J., Cui, J., Chen, D., Fang, Z., He, H., Ye, Z., Zhu, H., Wang, N., Wang, J., & Jin, Y. (2019). High-Efficiency Red Light-Emitting Diodes Based on Multiple Quantum Wells of Phenylbutylammonium-Cesium Lead Iodide Perovskites. ACS Photonics, 6(3), 587-594.

13. Jiang, Y., Wei, J., & Yuan, M. (2021). Energy-Funneling Process in Quasi-2D Perovskite Light-Emitting Diodes. The Journal of Physical Chemistry Letters, 12(10), 2593-2606.

14. Kong, L., Zhang, X., Li, Y., Wang, H., Jiang, Y., Wang, S., You, M., Zhang, C., Zhang, T., Kershaw, S. V., Zheng, W., Yang, Y., Lin, Q., Yuan, M., Rogach, A. L., & Yang, X. (2021). Smoothing the energy transfer pathway in quasi-2D perovskite films using methanesulfonate leads to highly efficient light-emitting devices. Nature Communications, 12(1), 1246.

15. Lee, J.-W., Dai, Z., Han, T.-H., Choi, C., Chang, S.-Y., Lee, S.-J., De Marco, N., Zhao, H., Sun, P., Huang, Y., & Yang, Y. (2018). 2D perovskite stabilized phase-pure formamidinium perovskite solar cells. Nature Communications, 9(1), 3021.

16. Li, Z., Chen, Z., Yang, Y., Xue, Q., Yip, H.-L., & Cao, Y. (2019). Modulation of recombination zone position for quasi-two-dimensional blue perovskite light-emitting diodes with efficiency exceeding 5%. Nature Communications, 10(1), 1027.

17. Li, Z.-T., Zhang, H.-W., Li, J.-S., Cao, K., Chen, Z., Xu, L., Ding, X.-R., Yu, B.-H., Tang, Y., Ou, J.-Z., Kuo, H.-C., & Yip, H.-L. (2022). Perovskite-Gallium Nitride Tandem Light-Emitting Diodes with Improved Luminance and Color Tunability. Advanced Science, 9(22), 2201844.

18. Liao, K., Li, C., Xie, L., Yuan, Y., Wang, S., Cao, Z., Ding, L., & Hao, F. (2020). Hot-Casting Large-Grain Perovskite Film for Efficient Solar Cells: Film Formation and Device Performance. Nano-Micro Letters, 12(1), 156.

19. Liu, J., Leng, J., Wu, K., Zhang, J., & Jin, S. (2017). Observation of Internal Photoinduced Electron and Hole Separation in Hybrid Two-Dimentional Perovskite Films. Journal of the American Chemical Society, 139(4), 1432-1435.

20. Liu, X., Zhang, Z., Lin, F., & Cheng, Y. (2021). Structural modulation and assembling of metal halide perovskites for solar cells and light-emitting diodes. InfoMat, 3(11), 1218-1250.

21. Liu, Z., Qiu, W., Peng, X., Sun, G., Liu, X., Liu, D., Li, Z., He, F., Shen, C., Gu, Q., Ma, F., Yip, H.-L., Hou, L., Qi, Z., & Su, S.-J. (2021). Perovskite Light-Emitting Diodes with EQE Exceeding 28% through a Synergetic Dual-Additive Strategy for Defect Passivation and Nanostructure Regulation. Advanced Materials, 33(43), 2103268.

22. Nah, Y., Solanki, D., Dong, Y., Röhr, J. A., Taylor, A. D., Hu, S., Sargent, E. H., & Kim, D. H. (2022). Narrowing the Phase Distribution of Quasi-2D Perovskites for Stable Deep-Blue Electroluminescence. Advanced Science, 9(24), 2201807.

23. Qin, C., Matsushima, T., Potscavage, W. J., Sandanayaka, A. S. D., Leyden, M. R., Bencheikh, F., Goushi, K., Mathevet, F., Heinrich, B., Yumoto, G., Kanemitsu, Y., & Adachi, C. (2020). Triplet management for efficient perovskite light-emitting diodes. Nature Photonics, 14(2), 70-75.

24. Quan, L. N., Yuan, M., Comin, R., Voznyy, O., Beauregard, E. M., Hoogland, S., Buin, A., Kirmani, A. R., Zhao, K., Amassian, A., Kim, D. H., & Sargent, E. H. (2016). Ligand-Stabilized Reduced-Dimensionality Perovskites. Journal of the American Chemical Society, 138(8), 2649-2655.

25. Ren, Z., Yu, J., Qin, Z., Wang, J., Sun, J., Chan, C. C. S., Ding, S., Wang, K., Chen, R., Wong, K. S., Lu, X., Yin, W.-J., & Choy, W. C. H. (2021). High-Performance Blue Perovskite Light-Emitting Diodes Enabled by Efficient Energy Transfer between Coupled Quasi-2D Perovskite Layers. Advanced Materials, 33(1), 2005570.

26. Shao, M., Bie, T., Yang, L., Gao, Y., Jin, X., He, F., Zheng, N., Yu, Y., & Zhang, X. (2022). Over 21% Efficiency Stable 2D Perovskite Solar Cells. Advanced Materials, 34(1), 2107211.

27. Taylor, A. D., Sun, Q., Goetz, K. P., An, Q., Schramm, T., Hofstetter, Y., Litterst, M., Paulus, F., & Vaynzof, Y. (2021). A general approach to high-efficiency perovskite solar cells by any antisolvent. Nature Communications, 12(1), 1878.

28. Tsai, H., Nie, W., Blancon, J.-C., Stoumpos, C. C., Asadpour, R., Harutyunyan, B., Neukirch, A. J., Verduzco, R., Crochet, J. J., Tretiak, S., Pedesseau, L., Even, J., Alam, M. A., Gupta, G., Lou, J., Ajayan, P. M., Bedzyk, M. J., Kanatzidis, M. G., & Mohite, A. D. (2016). High-efficiency two-dimensional Ruddlesden–Popper perovskite solar cells. Nature, 536(7616), 312-316.

29. Wu, C., Wu, T., Yang, Y., McLeod, J. A., Wang, Y., Zou, Y., Zhai, T., Li, J., Ban, M., Song, T., Gao, X., Duhm, S., Sirringhaus, H., & Sun, B. (2019). Alternative Type Two-Dimensional–Three-Dimensional Lead Halide Perovskite with Inorganic Sodium Ions as a Spacer for High-Performance Light-Emitting Diodes. ACS Nano, 13(2), 1645-1654.

30. Yang, D., Xie, C., Xu, X., You, P., Yan, F., & Yu, S. F. (2018). Lasing Characteristics of CH3NH3PbCl3 Single-Crystal Microcavities under Multiphoton Excitation. Advanced Optical Materials, 6(3), 1700992.

31. Yang, D., Zhao, B., Yang, T., Lai, R., Lan, D., Friend, R. H., & Di, D. (2022). Toward Stable and Efficient Perovskite Light-Emitting Diodes. Advanced Functional Materials, 32(9), 2109495.

32. Yang, R., Li, R., Cao, Y., Wei, Y., Miao, Y., Tan, W. L., Jiao, X., Chen, H., Zhang, L., Chen, Q., Zhang, H., Zou, W., Wang, Y., Yang, M., Yi, C., Wang, N., Gao, F., McNeill, C. R., Qin, T., Wang, J., & Huang, W. (2018). Oriented Quasi-2D Perovskites for High Performance Optoelectronic Devices. Advanced Materials, 30(51), 1804771.

33. You, M., Wang, H., Cao, F., Zhang, C., Zhang, T., Kong, L., Wang, L., Zhao, D., Zhang, J., & Yang, X. (2020). Improving Efficiency and Stability in Quasi-2D Perovskite Light-Emitting Diodes by a Multifunctional LiF Interlayer. ACS Applied Materials & Interfaces, 12(38), 43018-43023.

34. Zhang, L., Sun, C., He, T., Jiang, Y., Wei, J., Huang, Y., & Yuan, M. (2021). High-performance quasi-2D perovskite light-emitting diodes: from materials to devices. Light: Science & Applications, 10(1), 61.

35. Zhang, Q., Su, R., Du, W., Liu, X., Zhao, L., Ha, S. T., & Xiong, Q. (2017). Advances in Small Perovskite-Based Lasers. Small Methods, 1(9), 1700163.

36. Ting Xiang, Ting Li, Miaosheng Wang, Wei Zhang, Mahshid Ahmadi, Xiaoyan Wu, Tianfei Xu, Meiqin Xiao, Long Xu, Ping Chen. (2022). 12-Crown-4 ether assisted in-situ grown perovskite crystals for ambient stable light emitting diodes. Nano Energy, 95, 107000.

37. Zhang, Y., Sun, M., Zhou, N., Huang, B., & Zhou, H. (2020). Electronic Tunability and Mobility Anisotropy of Quasi-2D Perovskite Single Crystals with Varied Spacer Cations. The Journal of Physical Chemistry Letters, 11(18), 7610-7616.

38. Shang, Y. Q., Li, G., Liu, W. M., Ning, Z. J. (2018). Quasi-2D Inorganic CsPbBr3 Perovskite for Efficient and Stable Light-Emitting Diodes. Advanced Functional Material, 28(22), 1801193.

39. Zhuang, L., Wei, Q., Li, C., Ren, H., Li, Y., Shi, F., Zhai, L., Leng, K., Li, M., & Lau, S. P. (2022). Efficient Light-Emitting Diodes via Hydrogen Bonding Induced Phase Modulation in Quasi-2D Perovskites. Advanced Optical Materials, 10(21), 2201180.